Role of photoresponse of π electrons in light-driven DNA dissociations

Long Long Zhang*
The College of Physics and Optoelectronics, Taiyuan University of Technology, Taiyuan, 030024, China

Shi Jie Xie
School of Physics, Shandong University, Jinan 250100, China

Da Wei Kang
School of Physics and Engineering, Henan University of Science and Technology, Luoyang, 471003, China
(Received 18 April 2017; published 24 August 2017)

The role of photoresponse of π electrons in light-driven DNA dissociations is theoretically studied. A new model combining the Peyrard-Bishop-Dauxois model and the charge ladder model is first proposed. Then the evolutions of π-electronic states and H-bond stretching in the light-driven DNA dissociations are studied. The results show that light irradiation will induce ultrafast charge redistribution among bases, leading to the precursory insulator-to-metallic transition. This electronic transition will assist DNA to dissociate. Effects of screened Coulomb interactions on dissociation dynamics is emphatically discussed. Finally, it is also found that light-driven DNA dissociation preferentially occurs in the adenine-thymine–rich region rather than the guanine-cytosine–rich region.

DOI: 10.1103/PhysRevE.96.022414

1. INTRODUCTION

DNA has been proved powerful for use in nanotechnology because of its predictable nanometer-sized structures. One important example is that we can use DNA to develop the new two- and three-dimensional nanomachines by designing the nucleotide sequence [1,2]. To achieve this goal, people hope to control the dissociation and hybridization of DNA. Usually, by varying temperature [3,4], the ionic concentration, or pH value of the solvent [5,6], we can make the DNA duplex dissociate. However, these traditional approaches are costly and impossible for the practical design or organization of DNA nanostructures. Under such circumstances, light-regulated solutions come into play. Photon-induced RNA and DNA denaturation has early been experimentally detected by Hagen *et al.* [7]. In recent years, Asanuma *et al.* reported the fast realization of reversible photoregulation of DNA's dissociation and hybridization by introducing the photoresoponsive molecules azobenzene derivatives into DNA [8–10]. Azobenzene is one molecule that stabilizes in the *trans* pattern under visible light irradiation but the *cis* pattern under UV light irradiation. The *trans*-pattern azobenzene favors the duplex structure, whereas the *cis*-pattern azobenzene interrupts the H-bonding due to the steric effect and results in DNA dissociations. This photoinduced isomerization of azobenzene molecule acts as the driving force for the photoregulation of DNA nanomachines.

There are many advantages of using light in DNA-based nanomachines, e.g., we do not need other molecular fuels to drive DNA mechanical motion, so we can face fewer environmental problems [10]. However, because DNA can be taken as the π-electron stacked system [11], light irradiation will induce the redistribution of itinerant π electrons [12], which may play significant role in light-driven dissociations. Such a consideration sounds reasonable because people have found that electrostatic interactions between complementary bases play significant role in DNA's response to stretching [13]. Galindo and Sokoloff have also pointed out that two factors, the steric effect and the Coulomb interaction between charges of hydrogen-bonded pair, can both essentially affect the stability of the H-bond [5]. But, to date, few works have considered the effects of π electrons' Coulomb interactions on light-driven DNA dissociations, particularly in the presence of ionic solvent. To clarify this, we carry out the dynamical simulations of light-driven DNA dissociations. By studying the electronic and elastic evolutions after photoirradiation, the roles of π electrons in light-driven DNA dissociations are discussed.

Before starting the simulations, a suitable theoretical model should be considered first. The Peyrard-Bishop-Dauxois (PBD) model [14–20] has been proven to be powerful to theoretically describe the dynamics of thermal-driven DNA dissociations. The PBD model takes into account the Morse potential between the complementary bases and the nonlinear stacking interaction between the adjacent base pairs, so it is successful to give the experimental consistent thermal-driven dissociation curves [15–17]. But this model seems not so successful to deal with the itinerant electrons in DNA. On the other hand, we know that a so-called two-leg charge ladder (CL) model has been widely used in the study of charge transport in the DNA duplex [21–23]. We find that the CL model is also convenient to discuss the DNA dissociations, because it can effectively mimic the topology of double-stranded DNA. In this paper, we propose an alternative model combining the CL and PBD models and, therefore, it can simultaneously study the evolutions of π-electronic states and the mechanical motions of strands. Based on this model, the optical dynamical simulations of DNA dissociations are carried out. It is worth noting that both the CL model and PBD model ignore the angular degree of freedom. This simplification is equivalent to supposing that the prime factor

*zhanglonglong@tyut.edu.cn

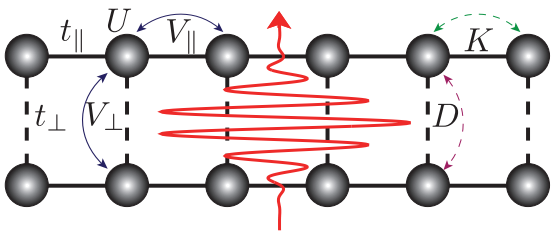

FIG. 1. Schematic view of the new model and the way of applying the incident laser pulse.

to determine the separation of the hydrogen-bonded base pair is the stability of the H-bond itself [5].

The remainder of this paper is organized as follows: In Sec. II, we introduce the model Hamiltonian and the dynamical calculating method; in Sec. III, we discuss the calculation results, where the screened Coulomb interaction effect and nucleotide sequence dependence on dissociation rate are emphatically discussed; in Sec. IV, we summarize our studies.

2. MODEL AND METHOD

A. The combined model of the CL and PBD models

The Hamiltonian which combines the CL and PBD models reads as follows (see Fig. 1 for the schematic view):

$$\mathcal{H} = \mathcal{H}_{\rm cl} + \mathcal{H}_{\rm PBD}, \tag{2.1}$$

where the CL-model part is

$$\begin{aligned}\mathcal{H}_{\rm cl} =& \sum_{j=1}^{2}\sum_{i}\epsilon_{j,i}(c_{j,i}^{\dagger}c_{j,i} + \text{H.c.}) \\ &- t_\parallel \sum_{j=1}^{2}\sum_{i}(c_{j,i}^{\dagger}c_{j,i+1} + \text{H.c.}) \\ &- t_\perp \sum_{i}\exp(-py_i)(c_{1,i}^{\dagger}c_{2,i} + \text{H.c.}) \\ &+ \frac{U}{4}\sum_{j=1}^{2}\sum_{i}n_{j,i}^2 + V_\parallel \sum_{j=1}^{2}\sum_{i}n_{j,i}n_{j,i+1} \\ &+ V_\perp \sum_{i}\exp(-xy_i)n_{1,i}n_{2,i}\end{aligned} \tag{2.2}$$

and the PBD-model part is

$$\begin{aligned}\mathcal{H}_{\rm PBD} =& + \sum_{i} D[\exp(-ay_i) - 1]^2 + \sum_{i}\frac{M}{2}\dot{y}_i^2. \\ &+ \sum_{i}\frac{K}{2}\{1 + \rho\exp[-c(y_i + y_{i-1})]\}(y_i - y_{i-1})^2.\end{aligned} \tag{2.3}$$

$\mathcal{H}_{\rm cl}$ describes the electronic structure, where $c_{j,i}^{\dagger}$ $(c_{j,i})$ indicates the π electron creation (annihilation) operator on base i of strand j; $\epsilon_{j,i}$ represents the on-site energy on base i of strand j; y_i represents the ith H-bond stretching; $t_\parallel$ represents the intrastrand hopping integral between the nearest-neighboring bases; and $t_\perp$ describes the intra-base-pair hopping integral [24–26]. The exponential function in the $t_\perp$ term with the cutoff constant p can describe the exponential tails of the H-bond wave functions during dissociation. In the vicinity of $y_i = 0$, the $t_\perp$ term returns to the Su-Schrieffer-Hegger–type [27] electron-phonon coupling. The value of p can be determined by matching to the *ab initio* calculations. In the following, it is adopted by $p = 0.2$ Å^{-1} [25].

For the Coulomb interaction $V_\perp$ between the complementary bases, the Debye-Hückel-screened Coulomb interaction with the inverse Debye screening length x is used [6,28–30]. It is worth noting that we have assumed that the bonds between the adjacent bases along the strand are rigid.

The PBD model Hamiltonian $\mathcal{H}_{\rm PBD}$ treats the mechanical energy classically, where the D term denotes the Morse potential describing the binding energy between the complementary bases; the K term describes the nonlinear stacking interaction between the adjacent base pairs, which can capture the long-range cooperative effect of nucleotide motions [15], and M denotes as the effective mass of a base pair.

The model used in this work, without taking into account the influence of temperature, is relevant to the low-temperature regime. We give the following parameters unless otherwise noted [18,21,22,31–33]: $t_\parallel = 0.2$ eV and $t_\perp = 0.15$ eV; $D = 0.04$ eV, $a = 4.45$ Å^{-1}; $K = 0.04$ eV/Å^2, M = 300 a.m.u.; $\rho = 0.5$, $c = 0.35$. Note that the ratio $t_\perp/t_\parallel = 0.75$ is relative larger than those in some references [31,34,35]. This is because in the extended ladder model in those references, diagonal hopping integrals are also taking into account, and the magnitude of the diagonal hopping integrals are approximately of the same order with or even greater than the intra-base-pair hopping integrals [34–37]. In our case, with no diagonal hopping integrals being considered, we compensate for this by taking a larger value of $t_\perp$ [33]. For Coulomb interactions, we set $U = 0.8$ eV, $V_\parallel = 0.6$ eV, and $V_\perp = 0.4$ eV, which leads to the charge-density-wave (CDW) ground state [21]. The size of DNA is set for $N = 100$ base pairs, and the periodical boundary condition is applied throughout the calculation. In the following calculations, we first consider the simplest case of homogeneous sequence. In this case, since the effect of ionization potential difference between the paired bases has been averagely renormalized into the Morse potential, we set the identical on-site energy for the bases for simplicity. One should be cautious in relating these parameters directly to the microscopic properties and recall that they arise as a result of several physical phenomena at the microscopic level.

B. The dynamical-simulation method

The effect of light on the π electron is simulated by adding a Peierls phase [38] on the hopping terms $c_{j,i}^{\dagger}c_{j,i+1}$. So the photon-electron interaction reads as

$$\mathcal{H}_E = - t_\parallel \sum_{j=1}^{2}\sum_{i}\left\{\exp\left[\frac{ier_0}{\hbar c}A(t)\right]c_{j,i}^{\dagger}c_{j,i+1} + \text{H.c.}\right\}, \tag{2.4}$$

where r_0 is the constant distance between the adjacent bases along the strand, the polarization of the incident pulse is set for along the strand direction, e and c are elementary electric charge and the light velocity, and the applied electric field $E(t)$

reads as

$$E(t) = -\partial A(t)/c\partial t. \tag{2.5}$$

$A(t)$ is the vector potential and given by

$$A(t) = A_0 \cos(\omega t)\, \exp\left[-\frac{(t-t_c)^2}{2\tau^2}\right], \tag{2.6}$$

where A_0, ω, t_c, and τ represents the amplitude, the oscillation frequency, the center, and the half-width of the pulse, respectively. The evolutions of the wave functions are obtained by stepwise integrating the Schrödinger equation,

$$i\hbar\dot{\Psi}_\mu(t) = H^{\rm HF}(t)\Psi_\mu(t), \tag{2.7}$$

where $\Psi_\mu(t)$ is the wave function vector, $H^{\rm HF}$ is the one-particle Hamiltonian by treating the many-body Coulomb interactions within the Hartree-Fock approximation $n_{j,i}n_{j,i+1} = n_{j,i}\langle n_{j,i+1}\rangle + n_{j,i+1}\langle n_{j,i}\rangle - \langle n_{j,i}\rangle\langle n_{j,i+1}\rangle$, where $\langle\,\rangle$ denotes a quantum average. Discretizing the time variable as $t_j = j\Delta t$ ($j = 0,1,2\cdots$) with the time variable Δt much smaller than optical phonon time scales, say, $\Delta t = 10^{-3}\sqrt{M/K} \approx 1$ fs, we integrate Eq. (2.7) step by step [39,40]:

$$\Psi_\mu(t_{j+1}) = \mathcal{T}\exp[-\frac{i}{\hbar}\int_{t_j}^{t_j+\Delta t} H^{\rm HF}dt]\Psi_\mu(t_j), \tag{2.8}$$

where $\mathcal{T}$ denotes the time-ordering operator.

The dynamics of the H-bond stretching are treated classically in Newtown's rule:

$$\begin{aligned} M\frac{d^2y_i}{dt^2} = F_i(t) &= \rho K\, \exp\{-c[y_{i+1}(t)+y_i(t)]\} \\ &\times [y_{i+1}(t)-y_i(t)] - \rho K\, \exp\{-c[y_{i-1}(t)+y_i(t)]\} \\ &\times [y_i(t)-y_{i-1}(t)] + \frac{c\rho K}{2}\exp\{-c[y_{i+1}(t)+y_i(t)]\} \\ &\times [y_{i+1}(t)-y_i(t)]^2 + \frac{c\rho K}{2}\exp\{-c \\ &\times [y_{i-1}(t)+y_i(t)]\}[y_i(t)-y_{i-1}(t)]^2 \\ &+K[y_{i-1}(t)+y_{i+1}(t)-2y_i(t)] + 2aD \\ &\times \exp[-ay_i(t)]\{\exp[-ay_i(t)]-1\} - 2pt_\perp \\ &\times \exp[-py_i(t)]|\langle c^\dagger_{1,i}c_{2,i}\rangle| + xV_\perp\exp[-xy_i(t)] \\ &\times \left(|\langle n_{1,i}n_{2,i}\rangle| - \frac{|\langle c^\dagger_{1,i}c_{2,i}\rangle|^2}{2}\right). \end{aligned} \tag{2.9}$$

With the discrete time variables, we evolve the H-bond stretching as

$$\begin{aligned} y_i(t_{j+1}) &= y_i(t_j) + \dot{y}_i(t_j)\Delta t, \\ \dot{y}_i(t_{j+1}) &= \dot{y}_i(t_j) + \frac{F_i(t_j)}{M}\Delta t. \end{aligned} \tag{2.10}$$

3. DISCUSSIONS

A. The screened Coulomb interaction effect

It has been indicated that DNA may have an uncertain number of itinerant π electrons [41]. In our calculations, the half-filling occupation is adopted. The equilibrium state of the duplex DNA is obtained by numerically integrating the Schrödinger equation [Eq. (2.7)] and solving the Newton's equation [Eq. (2.9)], meanwhile including the dissipative term $-M\gamma\frac{dy_n}{dt}$ ($\gamma = 10$ THz) [18]. After the structure being fully relaxed, the resultant electronic ground state turns out the CDW state with the optical gap about 2.3 eV, and the H-bond stretching is $y_i = 0$ in the equilibrium state [21,23].

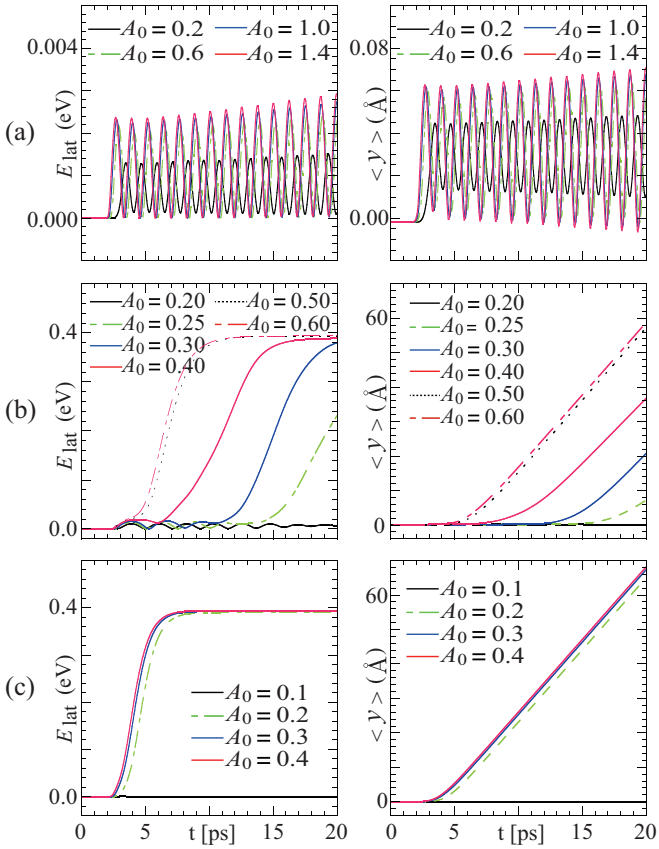

FIG. 2. Time evolutions of the mechanical energy (left column) and the averaged H-bond stretching $\langle y\rangle \equiv \sum_i y_i/N$ (right column) after the duplex DNA's ground state is photoexcited with various light intensity A_0 for different screening cases: (a) $x = 0.1$ Å^{-1}, (b) $x = 0.2$ Å^{-1}, and (c) $x = 0.3$ Å^{-1}, respectively. The unit of A_0 is $\frac{\hbar c}{er_0}$.

Then the incident laser pulse with the pulse width $2\tau = 1$ ps is applied. The frequency $\hbar\omega$ is set for the optical gap of the ground state. The intensity of the pulse is controlled by adjusting the pulse amplitude A_0. In the optical dynamical calculations, we initially set slight random distributions for $y_i(0)$ and $\dot{y}_i(0)$. The dissipative term is canceled in the optical dynamical calculations.

Figure 2 demonstrates the mechanical energy $E_{\rm lat}$ (left column) and the averaged H-bond stretching $\langle y\rangle = \sum_i y_i/N$ (right column) as functions of time t, in response to intensity-different laser pulses by varying A_0 and for different screened Coulomb interactions as $x = 0.1$ Å^{-1}, 0.2 Å^{-1}, and 0.3 Å^{-1}. The corresponding detailed information of the H-bond stretching $y_i(t)$ is further presented in Fig. 3.

In Fig. 2(a) for $x = 0.1$ Å^{-1}, double strands are strongly bound against light irradiation. Photons are absorbed to

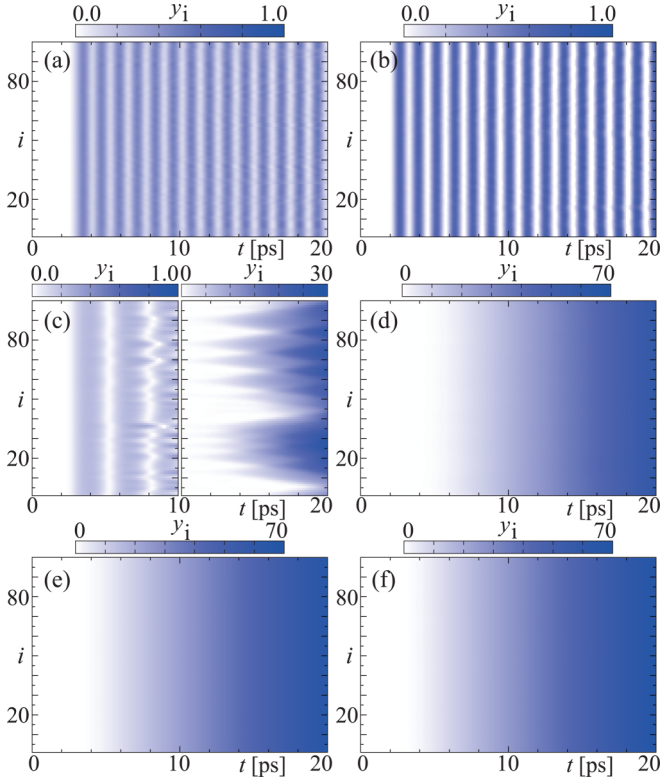

FIG. 3. H-bond stretching y_i as functions of time t and space index i for (a) $x = 0.1$ Å^{-1}, $A_0 = 0.2\ \frac{\hbar c}{er_0}$; (b) $x = 0.1$ Å^{-1}, $A_0 = 1.4\ \frac{\hbar c}{er_0}$; (c) $x = 0.2$ Å^{-1}, $A_0 = 0.3\ \frac{\hbar c}{er_0}$; (d) $x = 0.2$ Å^{-1}, $A_0 = 0.6\ \frac{\hbar c}{er_0}$; (e) $x = 0.3$ Å^{-1}, $A_0 = 0.2\ \frac{\hbar c}{er_0}$; (f) $x = 0.3$ Å^{-1}, $A_0 = 0.4\ \frac{\hbar c}{er_0}$, respectively.

induce the H-bond to oscillate in the composite potential well originated from the nonlinear stacking interaction and the Morse potential. When A_0 is larger than $0.6\ \hbar c/er_0$, the amplitude of the oscillations are saturated. The limiting energy transferred into the duplex backbone is dependent on the value of parameter p.

In Fig. 2(b) for $x = 0.2$ Å^{-1}, the light-driven DNA dissociation can be achieved when light intensity exceeds the threshold intensity $A_0 = 0.25\ \hbar c/er_0$. For instance, in the case of $A_0 = 0.3\ \hbar c/er_0$, the average value of H-bond stretching shows a precursory oscillation at first. The amplitude of the precursory oscillation is about 0.16 Å. At 11 ps, the local bubbles start to form at several distanced local sites. The size of these bubbles progressively increase, and then the bubbles merge with each other, causing the double strands to undergo a stepwise unzipping process. Similar formation and recombinations of the local bubbles have been widely reported in the thermal-driven DNA dissociation [32,42,43]. Increasing light intensity A_0 will lead to a faster realization of dissociation. For example, when $A_0 = 0.6\ \hbar c/er_0$, the double strands rapidly dissociate without local bubbles being formed [Fig. 3(d)]. In addition, we find that varying A_0 does not influence the mechanical energy of the final dissociated state. This is because the final dissociated state is stabilized on the plateau resulting from the Morse potential. In Fig. 2(c) for $x = 0.3$ Å^{-1}, as long as the light intensity is stronger than the

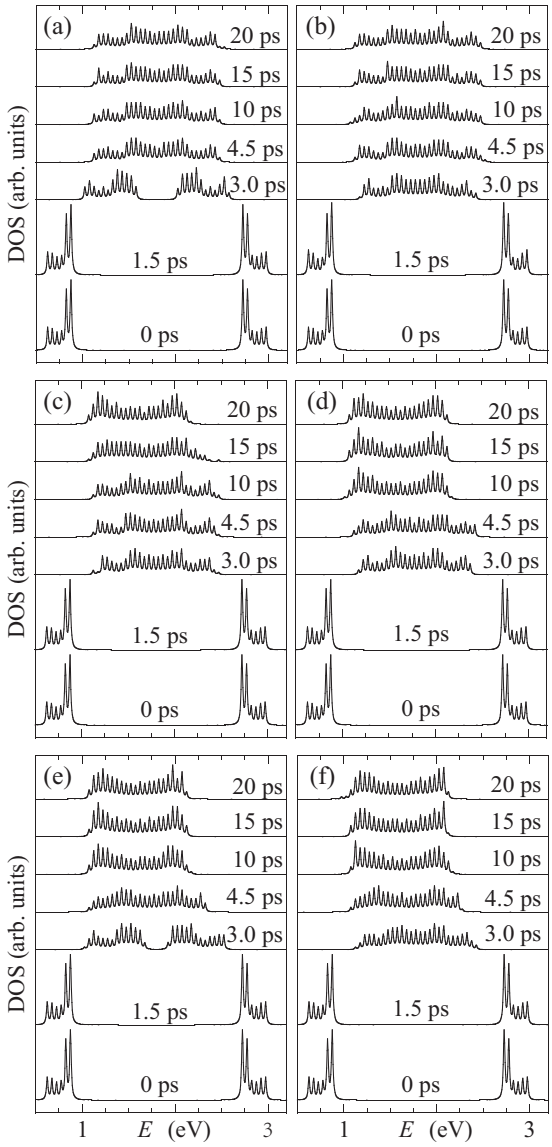

FIG. 4. Time-dependent density of states of π electrons with the same variable settings as in Fig. 3.

threshold, the dissociation of DNA is rapidly achieved without formations of local bubbles [Figs. 3(e) and 3(f)].

The above simulations indicate that the stronger screened Coulomb interaction assists light-driven DNA dissociations. This relationship between the dissociation rate and the screened Coulomb interactions is consistent with the case of thermal-driven DNA dissociation. For DNA in the low ion-concentrations conditions, the dissociation temperature decreases with increasing ion concentrations [5,6].

To understand the evolutions of π electronic states after photoirradiation, we present the corresponding snapshots of the time-dependent density of states (TDOS) of π electrons in Fig. 4. In Figs. 4(a) and 4(b), although DNA is not dissociated, the π electronic structure drastically changes. Fast charge redistributions among the bases immediately occur due to light irradiation, leading to the meltdown of CDW and closure of the band gap. This is nothing but the photoinduced insulator-to-metallic (PIIM) phase transition. In Figs. 4(c)–4(f), where

DNA is dissociated, PIIM is achieved before the dissociation of the double strands.

The dissociation rate variety under different screening conditions can be quantitatively analyzed from Eq. (2.9). The subtle competitions of forces in Eq. (2.9) influence the detailed DNA dissociation features. The last two terms are the driving forces relating to couplings between H-bond stretching and π electrons:

$$M\frac{d^2y_i}{dt^2}\infty\Big[-pt_\perp\exp[-py_i(t)](\langle c^\dagger_{1,i}c_{2,i}\rangle+\langle c^\dagger_{2,i}c_{1,i}\rangle)$$
$$+xV_\perp\exp[-xy_i(t)]\Big(\langle n_{1,i}\rangle\langle n_{2,i}\rangle-\frac{|\langle c^\dagger_{1,i}c_{2,i}\rangle|^2}{2}\Big)\Big]. \quad (3.1)$$

At the beginning stage of dissociation, fluctuations of H-bond stretching are first induced. The p force at the $y_i \approx 0$ stage behaves as an attractive force to draw back the separated base pairs; in contrast, the x force is repulsive, which assists the separation of base pairs, especially when π electronic state is metallic ($n_{1,i}=n_{2,i}=1; |\langle c^\dagger_{1,i}c_{2,i}\rangle| \approx 0.16$). It seems that the precursory realized PIIM is a necessary condition to trigger light-driven DNA dissociation.

In thermal-driven DNA dissociations, the heat energy induces the fluctuations of nucleotide bases and make the duplex backbone unstable. For light-driven DNA dissociations, the electron-phonon (e-p) coupling plays the important role. One can learn that the summation of the p term and x term relating to stretching y_i in Hamiltonian Eq. (2.2) can be taken as the effective e-p coupling, which acts as the bridge to transfer the absorbed photon energy from electrons into the duplex backbone.

Also, from a biological point of view, it is meaningful to discuss the threshold of the light energy for destruction of the genomic structure. We find that this threshold is strongly dependent on parameters p and x: first, both p and x act as the effective e-p coupling constant determining the efficiency of transferring the absorbed photon energy from electrons into duplex backbone; second, the stronger p tends to enhance the precursory photoinduced harmonic vibration of base pairs, while the stronger x tends to soften the harmonic vibration mode. Therefore, to achieve light-driven DNA dissociations, a stronger surrounding screening condition seems favorable. In this case, as long as the absorbed photon energy is able to trigger PIIM, the light-driven dissociation can be consequently realized.

B. Nucleotide sequence dependence

The above discussions have revealed the dynamical features of light-driven DNA dissociation and the conditions to achieve it. However, effects of bases' on-site energy on the dissociations are averaged out. Actually, the composition of the nucleotide sequence will significantly affect the electric conductance of DNA. In this section, we discuss the effect of concentrations of adenine-thymine (AT) and guanine-cytosine (GC) base pairs on the dissociations of a heterogeneous sequence.

We set the on-site energy as $\epsilon_A = -0.07$ eV, $\epsilon_T = 0.83$ eV, $\epsilon_G = -0.56$ eV and $\epsilon_C = 0.56$ eV [33,44]. The accurate on-site energies of the four nucleotide have also been elsewhere given by an *ab initio* method [45] and the linear combination of the atomic orbitals (LCAO) method [34]. We confirm the correctness of our parameters by clarifying that the energy differences among the four bases are consistent between ours and those in Refs. [34,45]. Morse potential parameters are set as $D_{AT} = 0.05$ eV, $a_{AT} = 4.2$ Å^{-1} for the AT base pairs and $D_{GC} = 0.075$ eV, $a_{GC} = 6.9$ Å^{-1} for the GC base pairs [20]. The solvent screening parameters are set for $x = 0.2$ Å^{-1}. The incident-light energy is set equal to the optical gap ($\hbar\omega = 2.8$ eV) and the pulse width is set for $2\tau = 1$ ps. In reality, the sequence can be of many different orders. For simplicity, we assume an AT-GC connected sequence as shown in Fig. 5. The base pairs from 1 to 50 are alternative AT base pairs, while the ones from 51 to 100 are GC base pairs.

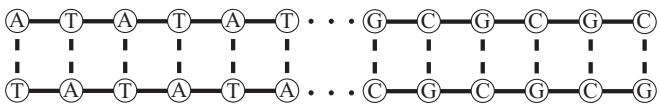

FIG. 5. Schematic view of a poly(dA)-poly(dT)- and poly(dG)-poly(dC)-connected heterogeneous sequence.

Figure 6 demonstrates light-driven dissociations in this AT-GC connected sequence. For $A_0 = 0.6\ \hbar c/er_0$ [Fig. 6(a)], which is beyond and close to the threshold light intensity, the local separation occurs around the 25th base pair (the center of the AT segment). The local separation proliferates to unzip the two strands, but it is hard to extend into the

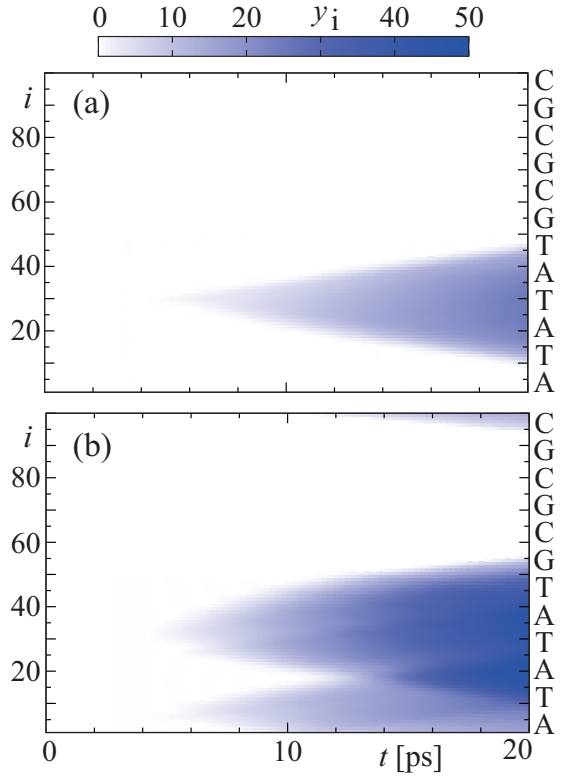

FIG. 6. H-bond stretching y_i as functions of time t and space index i for (a) $A_0 = 0.6\ \dfrac{\hbar c}{er_0}$ and (b) $A_0 = 1.0\ \dfrac{\hbar c}{er_0}$ for the heterogeneous sequence shown in Fig. 5.

GC segment. By increasing the intensity to $A_0 = 1.0\ \hbar c/er_0$ [Fig. 6(b)], more precursory local separations take place, and some GC base pairs close to the AT segment are also separated. In a word, photoirradiation preferentially separate the heterogeneous sequence in the AT-rich region rather than GC-rich region. In some previous work [19,32], the sequences with higher AT concentrations are easier to undergo thermal-driven DNA dissociations. The calculations in this paper well extend such a scenario to light-driven DNA dissociations. Because AT base pairs have a shallower potential well than the GC base pairs, it is easier for AT base pairs to reach the potential plateau when increasing the stretching of the H bonds. On the other hand, because CDW of a pure AT sequence has weaker charge alternations than that of a pure GC sequence, the minimum necessary photon intensity to induce the insulator-to-metal (I-M) phase transition in the pure GC sequence is about 1.5 times as high as that of the pure AT sequence. This conclusion is meaningful for designing the DNA-based nanomachines. By adjusting the concentrations and the relative locating positions of GC and AT base pairs, the light-driven DNA dissociation can be controlled.

4. SUMMARY

In summary, we have proposed one new model, which combines the PBD model and CL model, to study the optical dynamics of π electrons during light-driven DNA dissociations. As the Debye-Hückel screened Coulomb interaction and Slater-Koster type hopping $t_\perp$ between complementary bases are introduced, this model can give the reasonable electronic evolutions during DNA's dissociation process.

The calculation results show that there are indeed drastic electronic phase transitions on the light irradiation, and this photoresponse of π electrons can influence the light-driven DNA dissociation rate. Furthermore, increasing the solvent screening strength will assist DNA dissociations. This conclusion is consistent with Galindo and Sokoloff's early work for the salt ions effect on dissociation of hydrogen-bonded pair of negative point-charge ions [5], where a similar model including the Morse potential and the Debye-Hückel screened Coulomb interaction is used to describe the H-bonding potential energy. They discuss the thermal-driven hydrongen-bond dissociations and conclude that in the low-ion-concentration conditions, the dissociation temperature decreases with increasing ion concentrations. A similar scenario is reproduced in our work for light-driven DNA dissociations. Increasing the ionic concentrations will modify the the Morse potential shape and make the mean-force-potential well shallower. The incident light provides another two assistances: (1) the mean-force-potential well will be further shallowed due to photoinduced I-M phase transitions and (2) photon energy transferred to the backbone will overcome the mean-force-potential barrier in the photoinduced nonequilibrium process.

In addition, the effect of compositions of the nucleotide sequence on light-driven DNA dissociation is discussed. The calculation results indicate that, for a heterogeneous sequence, light-driven DNA dissociation prefers to occur in the AT-rich region rather than the GC-rich region, which is well consistent with the common knowledge in thermal-driven DNA dissociations.

Finally, it is worth noting that the present model dose not consider the nucleotide dependence on the intrastrand hopping integrals. An extended ladder model with accurate hopping integrals can be a candidate to refine our model in the future [34,36]. Also, the twisting effect is not considered in the present model, which is believed to be another essential factor affecting DNA dissociations [46]. The twisting effect can also bring many novel physics. For example, the double-helix structure of DNA leads to an internal magnetic field on the conduction electrons, therefore spin filtering effects in the DNA helix [47–49]. People can further improve the present study from the above aspects. We hope our present work has pointed out the potential important role played by the photoresponse of π electrons in light-driven DNA dissociations, and we look forward to attracting more and more theoretical and experimental interest.

ACKNOWLEDGMENT

This work was supported by the National Natural Science Foundation of China (Grants No. 11174181 and No. 11204066).

[1] N. C. Seeman, Nature **421**, 427 (2003).
[2] J. Bath and A. J. Turberfield, Nat. Nanotechnol. **2**, 275 (2007).
[3] R. M. Wartell and A. S. Benight, Phys. Rep. **126**, 67 (1985).
[4] G. Altan-Bonnet, A. Libchaber, and O. Krichevsky, Phys. Rev. Lett. **90**, 138101 (2003).
[5] C. E. Galindo and J. B. Sokoloff, Phys. Rev. E **48**, 3091 (1993).
[6] S. A. Hassen, F. Guarnieri, and E. L. Mehler, J. Phys. Chem. B **104**, 6478 (2000).
[7] U. Hagen, K. Keck, H. Kröger, H. Zimmermann, and T. Lücking, Biochim. Biophys. Acta **95**, 418 (1965).
[8] H. Asanuma, X. G. Liang, T. Yoshida, and M. Komiyama, ChemBioChem. **2**, 39 (2001).
[9] X. G. Liang, T. Mochizuki, T. Fuji, H. Kashida, and H. Asanuma, Nat. Comput. **11**, 231 (2012).
[10] Y. Kamiyama and H. Asanuma, Acc. Chem. Res. **47**, 1663 (2014).
[11] D. B. Hall, R. E. Holmlin, and J. K. Barton, Nature **382**, 731 (1996).
[12] M. Ratner, Nature **397**, 480 (1999).
[13] A. V. Tkachenko, Phys. Rev. E **74**, 041801 (2006).
[14] M. Peyrard and A. R. Bishop, Phys. Rev. Lett. **62**, 2755 (1989).
[15] T. Dauxois, M. Peyrard, and A. R. Bishop, Phys. Rev. E **47**, R44(R) (1993).
[16] Y. l. Zhang, W.-M. Zheng, J.-X. Liu, and Y. Z. Chen, Phys. Rev. E **56**, 7100 (1997).
[17] A. Campa and A. Giansanti, Phys. Rev. E **58**, 3585 (1998).
[18] S. Komineas, G. Kalosakas, and A. R. Bishop, Phys. Rev. E **65**, 061905 (2002).

[19] G. Kalosakas, K. Ø. Rasmussen, and A. R. Bishop, Syn. Meta. **141**, 93 (2004).
[20] J.-X. Zhu, K. Ø. Rasmussen, A. V. Balatsky, and A. R. Bishop, J. Phys.: Condens. Matter **19**, 136203 (2007).
[21] J. Yi, Phys. Rev. B **68**, 193103 (2003).
[22] R. Gutiérrez, S. Mohapatra, H. Cohen, D. Porath, and G. Cuniberti, Phys. Rev. B **74**, 235105 (2006).
[23] E. Díaz, A. V. Malyshev, and F. Domínguez-Adame, Phys. Rev. B **76**, 205117 (2007).
[24] J. C. Slater and G. F. Koster, Phys. Rev. **94**, 1498 (1954).
[25] R. G. Endres, D. L. Cox, and R. R. P. Singh, Rev. Mod. Phys. **76**, 195 (2004).
[26] A. Gross, M. Scheffler, M. J. Mehl, and D. A. Papaconstantopoulos, Phys. Rev. Lett. **82**, 1209 (1999).
[27] W. P. Su, J. R. Schrieffer, and A. J. Heeger, Phys. Rev. Lett. **42**, 1698 (1979).
[28] G. Ramachandran and T. Schlick, Phys. Rev. E **51**, 6188 (1995).
[29] H. M. Harreis, C. N. Likos, and H. Löwen, Biophys. J. **84**, 3607 (2003).
[30] J. J. Jones, J. R. C. van der Maarel, and P. S. Doyle, Phys. Rev. Lett. **110**, 068101 (2013).
[31] H. Mehrez and M. P. Anantram, Phys. Rev. B **71**, 115405 (2005).
[32] S. Ares, N. K. Voulgarakis, K. Ø. Rasmussen, and A. R. Bishop, Phys. Rev. Lett. **94**, 035504 (2005).
[33] S. Kundu and S. N. Karmaker, AIP Advances **5**, 107122 (2015).
[34] L. G. D. Hawke, G. Kalosakas, and C. Simserides, Eur. Phys. J. E **32**, 291 (2010).
[35] K. Senthikumar, F. C. Grozema, C. F. Guerra, F. M. Bickelhaupt, F. D. Lewis, Y. A. Berlin, M. A. Ratner, and L. D. A. Siebbeles, J. Am. Chem. Soc. **127**, 14894 (2005).
[36] K. Lambropoulos, M. Chatzieleftheriou, A. Morphis, K. Kaklamanis, R. Lopp, M. Theodorakou, M. Tassi, and C. Simserides, Phys. Rev. E **94**, 062403 (2016).
[37] A. A. Voityuk, N. Rösch, M. Bixon, and J. Jortner, J. Phys. Chem. B **104**, 9740 (2000).
[38] G. De Filippis, V. Cataudella, E. A. Nowadnick, T. P. Devereaux, A. S. Mishchenko, and N. Nagaosa, Phys. Rev. Lett. **109**, 176402 (2012).
[39] K. Yonemitsu and N. Miyashita, Phys. Rev. B **68**, 075113 (2003).
[40] S. Yamamoto and J. Ohara, J. Phys.: Condens. Matter **20**, 415215 (2008).
[41] X.-T. Gao, X. Fu, L.-M. Mei, and S.-J. Xie, J. Chem. Phys. **124**, 234702 (2006).
[42] Y. Zeng, A. Montrichok, and G. Zocchi, Phys. Rev. Lett. **91**, 148101 (2003).
[43] Y. Zeng, A. Montrichok, and G. Zocchi, J. Mol. Biol. **339**, 67 (2004).
[44] A.-M. Guo, S.-J. Xiong, Z. Yang, and H.-J. Zhu, Phys. Rev. E **78**, 061922 (2008).
[45] H. Sugiyama and I. Saito, J. Am. Chem. Soc. **118**, 7063 (1996).
[46] M. Barbi, S. Cocco, and M. Peyrard, Phys. Lett. A **253**, 358 (1999).
[47] G. L. J. A. Rikken, Science **331**, 864 (2011).
[48] A.-M. Guo and Q.-f. Sun, Phys. Rev. Lett. **108**, 218102 (2012).
[49] T.-R. Pan, A.-M. Guo, and Q. F. Sun, Phys. Rev. B **92**, 115418 (2015).